Differential default-mode network effective connectivity in young-onset Alzheimer's disease variants

Seda Sacu[1], Catherine F. Slattery[2], Karl J. Friston[3], Ross W. Paterson[2], Alexander J.M. Foulkes[2], Keir Yong[2], Sebastian Crutch[2], Jonathan M. Schott[2], Adeel Razi[3,4,5]

Author Affiliations:

[1] Central Institute of Mental Health, Medical Faculty Mannheim, University of Heidelberg, Mannheim, Germany

[2] Department of Neurodegenerative Disease, Institute of Neurology, University College London, London, UK

[3]Wellcome Centre for Human Neuroimaging, Institute of Neurology, University College London, London, United Kingdom

[4] Turner Institute for Brain and Mental Health, School of Psychological Sciences, Monash University, Clayton, Australia

[5] CIFAR Azrieli Global Scholars Program, CIFAR, Toronto, Canada

Correspondence to: Adeel Razi

Turner Institute for Brain and Mental Health, School of Psychological Sciences, Monash University, Australia

Clayton VIC 3800

Email: adeel.razi@monash.edu

Abstract

Young-onset Alzheimer's Disease is a rare form of Alzheimer's Disease characterized by early symptom onset (< 65 years) and heterogeneous clinical phenotypes. Previous studies have consistently shown that patients with late-onset Alzheimer's exhibit alterations in the default-mode network—a large-scale brain network associated with self-related processing and autobiographical memory. However, the functional organization of the default-mode network is far less clear in young-onset Alzheimer's disease. Here, we assessed default-mode network effective connectivity in two common young-onset Alzheimer's disease variants (i.e., typical amnestic variant and posterior cortical atrophy) and healthy participants to identify disease- and variant-specific differences in the default-mode network.

This case-control study was conducted with thirty-nine young-onset Alzheimer's disease patients, including typical amnestic (n = 26, 15 females, mean age = 61) and posterior cortical atrophy (n = 13; 8 females, mean age = 61.8), and 24 age-matched healthy participants (13 females, mean age=60.1). All participants underwent resting-state functional MRI and extensive neuropsychological testing. Spectral dynamic causal modelling was performed to quantify resting-state effective connectivity between default-mode network regions. Parametric empirical Bayes analysis was then performed to characterise group differences in effective connectivity.

Our results showed that patients with typical Alzheimer's disease variant showed increased connectivity from medial prefrontal cortex to posterior default-mode network nodes as well as reduced inhibitory connectivity from hippocampus to other default-mode network nodes, relative to healthy controls. Patients with posterior cortical atrophy exhibited decreased connectivity from posterior cingulate cortex to medial prefrontal cortex and bilateral angular gyrus and reduced inhibitory connectivity from left hippocampus to other default-mode network nodes compared to healthy controls. Right hippocampus connectivity differentiated the two patient groups. Patients with typical Alzheimer's disease variant had lower inhibitory connectivity from right hippocampus to other default-mode network nodes than the patients with posterior cortical atrophy.

Our findings suggest that resting-state default-mode network connectivity is a physiological phenotype of young-onset Alzheimer's disease that could contribute to a new understanding of functional integration in this condition.

Introduction

Young-onset Alzheimer's Disease (AD, symptom-onset< 65 years) is a rare form of AD which constitutes 5% of all AD cases [1]. Similar to late-onset AD, most patients diagnosed with young-onset AD present with memory deficits and prominent medial temporal lobe atrophy [1]. However, the clinical profile in young-onset AD is more heterogeneous than late-onset AD [2,3]. A higher proportion of the patients present with atypical phenotypes characterized by other focal symptoms than memory [4,5]. Posterior cortical atrophy (PCA) is the most common atypical phenotype dominated by visuoperceptual/visuospatial problems, parieto-occipital atrophy and relatively preserved episodic memory [6]. Despite the shared pathology, there are remarkable differences between two young-onset AD phenotypes in terms of grey matter volume, glucose hypometabolism and organization of large-scale brain networks [1,5].

There is a growing literature investigating large-scale brain networks to understand cognitive and affective dysfunctions in neurological disorders [7]. The default-mode network (DMN) is one of the most studied large-scale intrinsic brain networks, which comprises the posteromedial cortex (posterior cingulate cortex and precuneus), medial prefrontal cortex, angular gyrus, and medial temporal lobe. DMN is preferentially activated when individuals engage with internally driven processes such as perspective taking, autobiographical memory, future planning and self-awareness [8]. The importance of the DMN in AD research is twofold. First, the activity of the DMN shows a striking correlation with the topography of amyloid β (Aβ) deposition in AD patients [9]. Second, the activity of the DMN is correlated with self-referential thoughts and episodic memory, indicating that memory impairment identified in AD can be attributable to disrupted DMN connectivity [9].

The majority of previous connectivity studies were conducted in patients with late-onset AD. Their results indicate that patients with late-onset AD showed decreased local connectivity in the DMN [10,11] and decreased connectivity between the DMN regions, especially between posterior cingulate cortex and other default-mode network nodes [12–15] Compared to late-onset

AD, a relatively small number of connectivity studies investigated differences in large-scale networks in patients with young-onset AD. These studies reported both increased [16] and decreased functional connectivity between the DMN regions in patients with young-onset AD [16–18] . Only a few studies investigated DMN connectivity in young-onset AD variants [19,20]. Lehmann *et al.*, (2015) identified increased anterior DMN functional connectivity in typical AD and PCA compared to controls, whereas the other study found decreased DMN functional connectivity in the PCA variant compared to controls [20]. However, none of these studies examined directed (i.e., effective) connectivity in the DMN in patients with young-onset AD or young-onset AD variants.

In this work, we aimed to investigate effective connectivity between the DMN nodes in young-onset AD variants (i.e., typical AD and PCA) and healthy age-matched controls using dynamic causal modelling (DCM). We hypothesized that patients with young-onset AD would show decreased connectivity in the DMN compared to healthy controls. In addition, based on structural and functional differences between the two AD variants, we expected to see group differences in the DMN connectivity between the two patient groups. We hypothesized that patients with typical AD would show more impairment in the connectivity of memory and self-related processing regions, such as hippocampus and medial prefrontal cortex, whereas patients with PCA would show aberrant connectivity involving parietal regions, such as the angular gyrus and posterior cingulate cortex.

Materials and methods

Participants

The case-control study included forty-five patients with probable AD [21] with symptom onset < 65 years and 24 age-matched healthy individuals. The participants were recruited between 2013 and 2015 from Cognitive Disorders Clinic at the National Hospital for Neurology and Neurosurgery. Patients were classified based on their leading symptoms as having typical amnestic [21] or atypical (PCA) AD phenotype [22]. Patients with an autosomal dominant mutation (n=1) or other atypical AD phenotypes (n = 3; two patients with logopenic progressive aphasia and one patient with behavioural/dysexecutive AD phenotype) were excluded from the study. Furthermore, two patients were excluded from further analyses due to excessive head motion (> 3 mm in translation or 3 degrees in rotation parameters). The final sample included 26 patients with typical AD, 13 patients with PCA and 24 healthy controls (See Table 1 for sample characteristics). Groups were matched in terms of age, sex, education, and handedness. However, there was a significant group difference in head motion quantified by using frame-wise displacement [23]. Patients with typical AD had significantly higher head motion than healthy controls ($t = -0.32$, $p = 0.03$). Patient groups did not differ in terms of disease severity and duration.

The study was approved by the National Hospital for Neurology and Neurosurgery Research Ethics Committee. All participants provided written informed consent.

Table 1. Sample Characteristics.

	TAD (n= 26)	PCA (n=13)	HC (n=24)	p
Demographics				
Age, mean (SD)	61 (5.1)	61.8 (5.2)	60.1 (5.7)	0.62
Sex, n, male/female	12/14	5/8	11/13	0.88
CSF consistent with AD*	25/26	11/13		
Education, mean (SD)	15 (3)	14.9 (2.5)	16.7 (3)	0.10
Handedness, n, R/L	25/1	12/1	21/3	0.52
Head motion, mean (SD)	0.9 (0.5)	0.7 (0.4)	0.6 (0.4)	**0.03**
Age at onset, mean (SD)	56 (4.4)	56.5 (4.3)		0.72
Disease duration, mean (SD)	5.6 (2.8)	6 (3.3)		0.73
Neuropsychological Tests				
MMSE, median (IQR)	21 (8)	22 (8)	30 (1)	< **0.001** [a]
RMT, median (IQR)	38 (8.7)	39.4 (9.5)	50 (1.7)	< **0.001** [a]
GDA, median (IQR)	1 (5)	1 (4.5)	15 (11.7)	< **0.001** [a]
GDST, median (IQR)	28 (19.4)	25 (17.2)	53 (9.5)	< **0.001** [a]
VOSP, median (IQR)	59.5 (18.7)	43 (18.4)	67 (2.7)	< **0.001** [a]
DKEFS, median (IQR)	4 (3)	2.8 (7)	11 (5)	< **0.001** [a]

* Aβ1-42 <627 pg/ml and/or Tau/ Aβ1-42 ratio >.52.

Missing values per variable: RMT (n=1), GDA (n=2), GDST (n=4), VOSP (n=3), DKEFS (n=3)

Cognitive measurements

All participants underwent an extensive neuropsychology test battery to measure the severity of cognitive impairment (Mini-Mental State Examination [MMSE][24]), episodic

memory (Recognition Memory Test [RMT][25]), numeracy and literacy respectively (Graded Difficulty Arithmetic [GDA][26]) and Graded Difficulty Spelling Test [GDST][27]], visuospatial and visuoperceptual performance (Visual Object and Spatial Perception [VOSP] [28] battery) and speed of processing and executive functions (Delis-Kaplan Executive Function System [DKEFS][29]). All cognitive measurements were continuous. For all scales, higher scores indicated higher cognitive performance.

As expected, patient groups had significantly lower scores in MMSE and all neuropsychological tests than the control group ($p < 0.001$, See Table 1). Patients with PCA had lower scores in VOSP than the patients with typical AD ($p < 0.05$). Patient groups did not significantly differ in other neuropsychological tests. There was no significant group difference in MMSE, disease onset, and disease duration between the two patient groups.

Data acquisition and preprocessing

The data were acquired on a Siemens Magnetom Trio (Siemens, Erlangen, Germany) 3T MRI scanner using a 32-channel phased array head coil. Structural images were obtained using a sagittal magnetization-prepared rapid gradient echo (MP-RAGE) three-dimensional T1-weighted sequence (TE = 2.9 ms, TR = 2200 ms, TI = 900 ms, flip angle = 10°, FoV = 282 × 282 mm, 208 slices with 1.1×1.1×1.1 mm voxels). Functional images were obtained using an asymmetric gradient echo echo-planar sequence sensitive to blood oxygen level-dependent contrast (TE= 30 ms, TR = 2200 ms, flip angle = 80°, FoV = 212 × 212 mm, voxel size = 3.3 × 3.3 × 3.3 mm). Whole brain coverage for the functional data was obtained using 36 contiguous interleaved 3.3 mm transversal slices, acquired parallel to the plane transecting the anterior and posterior commissure (AC-PC plane). In total, 140 volumes were acquired during the resting state scan. Before the resting state scan subjects were instructed to simply rest in the scanner with their eyes open while staying as still as possible.

Preprocessing steps were performed using SPM12. The initial five volumes were discarded to allow for equilibration of the magnetic field. Slice acquisition dependent time shifts were corrected per volume. All volumes were realigned to the first volume using a six-parameter (rigid body) linear transformation to correct within subject head motion. The resulting images were then spatially normalised to a standard brain template in the MNI coordinate space. Data were resampled to 3-mm isotropic voxels and spatially smoothed using a 6-mm full-width half-maximum (FWHM) Gaussian kernel. Six motion parameters and time series from white matter and cerebrospinal fluid were used as nuisance regressors for physiological noise correction.

The regions of interest selection

Constrained independent component analysis (ICA) was performed to identify the network of interest using the Group ICA of fMRI Toolbox (https://trendscenter.org/software/gift/). Constrained ICA is a semi-blind dimension reduction method that identifies an independent component in subject data, which matches with the supplied spatial references [30]. This approach features two main advantages. First, it eludes problems with subjective component selection [31]. Second, the resulting components have higher signal-to-noise ratio than the standard ICA approaches. Application of constrained ICA has been previously used to identify regions of interest for dynamic causal modelling (DCM) analysis [31–34].

A pre-existing template for DMN (dorsal DMN) [35] was used as a spatial reference for constrained ICA. A one-sample t-test was performed to obtain group-level peak coordinates for regions of interest (ROIs). Based on the t-test results ($p < 0.05$, family-wise error (FWE) corrected), we selected following ROIs for subsequent DCM analysis: medial prefrontal cortex (mPFC; x=-6, y=53, z=17), posterior cingulate cortex (PCC; x=6, y=-55, z=29), bilateral angular gyrus (ANG; left: x=-48, y=-67, z=35 ; right: x=48, y=-61, z=29) and bilateral hippocampus (HPC; left: x=-24, y=-25, z=-13; right: x=27, y=-25, z=-10). These coordinates

are very similar to the anatomical locations reported by a coordinate-based meta-analysis of DMN in healthy adults and AD patients [36]. ROI time series were defined as the first principal component from all voxels within in a 8 mm radius sphere centred on the group maximum of each node [37]. Subject-specific whole brain mask and MNI-based ROI masks were used to ensure that regional responses were based on voxels within the anatomical boundaries of the brain and specific ROI.

Finally, we conducted a one-way ANOVA to see any of the selected ROIs of the DMN component shows group differences—in the amplitude of fluctuations in each ROI—between typical AD, PCA and healthy controls.

Data analysis

Statistical analysis

Statistical analysis was performed in SPSS 24 (SPSS Inc., Chicago, Illinois, USA). A nominal significance threshold was set at p=0.05. Chi-squared tests were performed to identify if sex and handedness were equally distributed across groups. A one-way ANOVA was performed to compare age, education, neuropsychological test scores, and mean head motion between groups. Non-parametric ANOVA test (Kruskal-Wallis) was used for the same purpose when parametric assumptions were not met. Two-sample t tests were then performed to compare two patient groups in terms of disease duration and age at onset.

Spectral dynamic causal modelling

The spectral DCM implemented in the SPM12 (DCM 12.5, revision 7497) was performed to estimate effective connectivity during resting-state. Spectral DCM estimates resting-state connectivity by fitting observed complex fMRI cross spectra. It finds the best effective connectivity among the hidden neuronal states that explains functional connectivity among haemodynamic responses [37–39]. Here, we set a fully connected model (6 x 6 = 36 connection parameters) to compare all possible nested models within the network [40]. After the model

estimation, we performed diagnostics to check the quality of the DCM model fitting to ensure that model inversion was successful [41]. All participants had more than 60% explained variance by the model (M = 89.5, SD = 3.9).

Parametric empirical bayes

A parametric empirical Bayes (PEB) analysis was then performed at the group level to estimate the group mean and group differences in effective connectivity [40]. PEB in this setting entails a general linear model (GLM) of between-subject (random) effects that best explain the within-subject (DCM) estimates of connectivity. Bayesian Model Reduction (BMR) was used to prune connection parameters from the full PEB model until there was no further improvement in model-evidence (based on log-evidence or free energy). The parameters of reduced models were then averaged and weighted by their model evidence by Bayesian Model Averaging (BMA) to account for any uncertainty over reduced models: i.e., the parameters under each reduced model were averaged after weighting by the evidence (a.k.a., marginal likelihood) of the model under which they were estimated.

Due to the group differences in head motion, we included mean framewise displacement in the analysis as a covariate of no interest at the between the subject level. All inferences were made using a posterior probability criterion of 95% (equivalent of a strong evidence) for each connection. In other words, the model evidence or marginal likelihood of a model with a particular parameter was 20 times greater than the corresponding model in which the parameter was removed.

Brain-behaviour relationship

To reduce the number of statistical comparisons, we conducted a principal component analysis using MMSE, RMT, GDA, GDST, VOSP, and DKEFS sum scores (See Supplementary Material S4 for details). Missing values were handled using expectation-

maximization approach. Only one component—which explained 68% of the variance—was identified. The component score was then used to test for an association between the group-specific DMN connectivity and cognitive performance within the PEB framework. All inference was made using a posterior probability criterion of 95% (equivalent of strong evidence) for each connection.

Replication analysis

Here, we used the dorsal DMN component as a spatial reference—or constraint—for the ICA analysis, since it covers most reliable DMN regions, such as PCC, medial PFC and angular gyrus [36] as well as hippocampus—an important brain region for AD pathology [42] but less consistently reported across the studies [36]. Although DMN is mostly treated as a homogenous network, several studies have identified distinct components within DMN [35,43,44]. Furthermore, some studies have shown that certain DMN components were differentially altered in AD [11,19,45]. Therefore, we also included another DMN component called ventral DMN [35] to see if our results are specific to the chosen component or young-onset AD pathology.

We therefore applied constrained ICA to identify subject-specific ventral DMN component, and a one-sample *t* test was performed to identify the peak coordinates for ROIs. To keep the model as similar as possible, we included the following ROIs in a spectral DCM analysis: precuneus, bilateral middle frontal gyrus, bilateral parahippocampal gyrus and bilateral angular gyrus. The coordinates and group-level component map can be found in the Supplementary Material (Supplementary Table S1, Supplementary Fig. S1). In an equivalent manner, a fully connected model was set at the first level and group differences were estimated within the PEB framework. The results of this replication analysis are summarised in the discussion.

Results

Independent component analysis

A component representing dorsal DMN was identified across participants using constrained ICA (Figure 1). Within this component, we found a group difference between typical AD and healthy controls. YOAD patients with typical phenotype showed lower PCC activation (as measured by the amplitude of fluctuations in BOLD signal) compared to healthy controls ($p < 0.05$, cluster-level FWE-corrected; Supplementary Fig. S2). However, this result did not survive at whole-brain corrected level. No group difference was found for any ROI within the ventral DMN component.

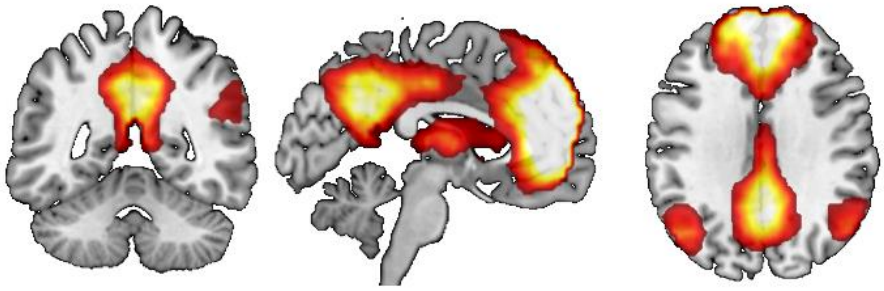

Figure 1. Default-mode network component identified using constrained independent component analysis (p <0.05, FWE-corrected at whole-brain).

Dynamic causal modelling

Group means

Group specific effective connectivity matrices for dorsal DMN are shown in Figure 2 (see Supplementary Fig. S4 for the ventral DMN component). Two types of connection can be seen in Figure 2: excitatory and inhibitory (extrinsic or between-region) connections. An excitatory connection means that the activity of the source region leads to increases in the activity of the target region, whereas an inhibitory connection means that the activity of the source region leads to decreases in the activity of the target region [46]. Independent from the sign (negative or

positive), self-connections (e.g., PCC → PCC) should be read as inhibitory because (intrinsic or within-region) self-connections are log-scaled. A positive self-inhibitory connection indicates a more inhibited region, which is less responsive to the input, while a negative self-inhibitory connection indicates a less inhibited region resulting in disinhibition to afferent input [47].

The groups showed a mixed pattern of excitatory and inhibitory connections within DMN. However, outgoing connections from HPC to other DMN regions were inhibitory across all groups, while interhemispheric HPC connections were excitatory. Missing entries correspond to redundant connections that have been removed following Bayesian model reduction (that did not differ from their prior expectation).

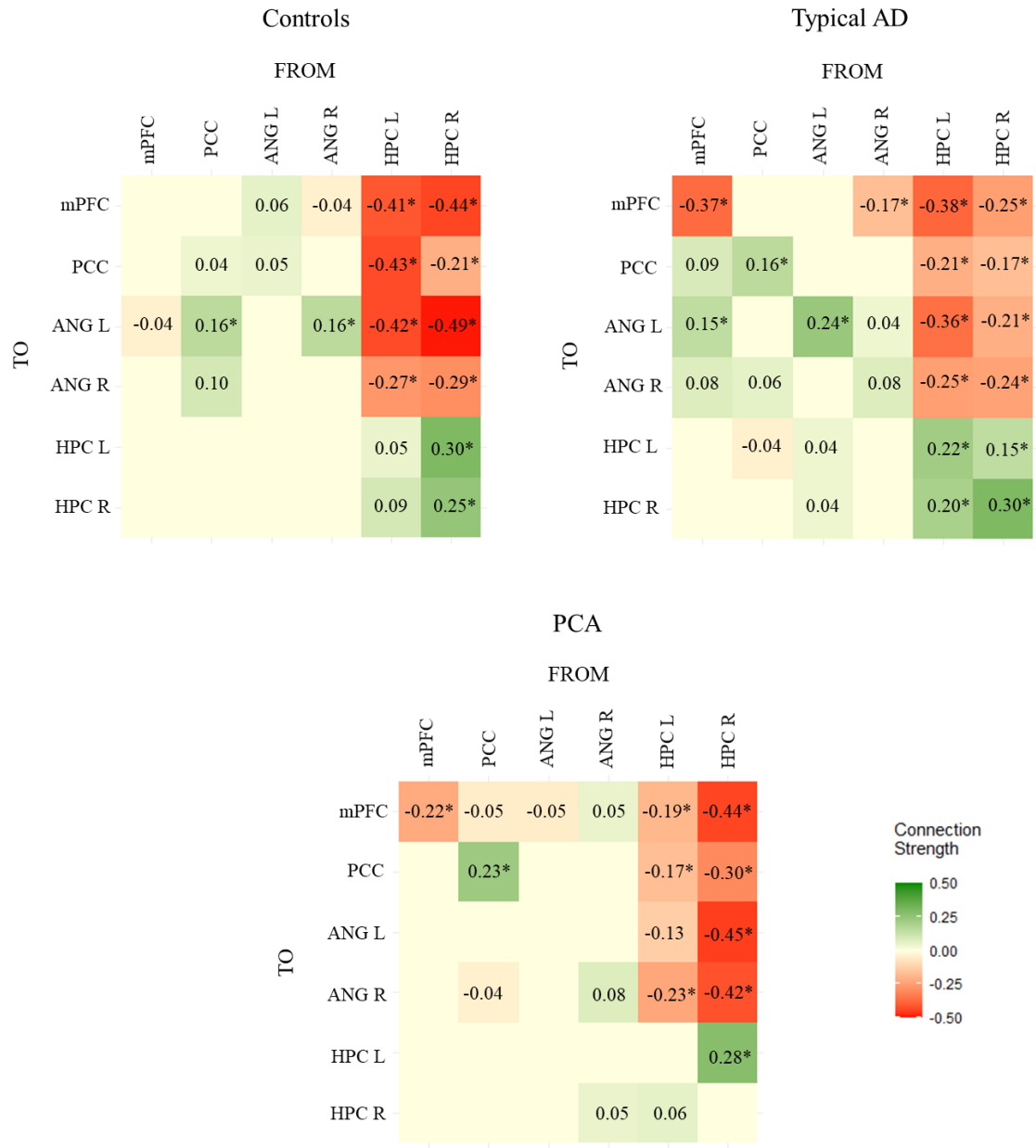

Figure 2. Mean effective connectivity within the DMN. Green colour represents excitatory connections, whereas red colour represents inhibitory connections. Self-connections should be interpreted as inhibitory, irrespective of the colour. Connections with strong evidence [i.e., *posterior probability* > 0.95] are marked with an asterisk. Abbreviations: ANG, angular gyrus; HPC, hippocampus; mPFC, medial prefrontal cortex; PCC, posterior cingulate cortex.

Group differences

Typical AD versus healthy controls

Compared to the healthy controls, patients with typical AD showed lower mPFC self-connection indicating higher input sensitivity of the region in the disease group (Figure 3). In addition, patients with typical AD had higher connectivity from mPFC to posterior DMN regions (i.e., PCC and bilateral ANG) than the healthy controls. The patient group exhibited excitatory connections from mPFC to posterior DMN regions, which were missing in the healthy group. Contrary to the mPFC self-connection, left ANG self-connection was higher in the patient group indicating the lower input sensitivity of the region. Additionally, patients with typical AD variant showed lower inhibitory connectivity from left HPC to PCC and from right HPC to mPFC and left ANG than the healthy controls.

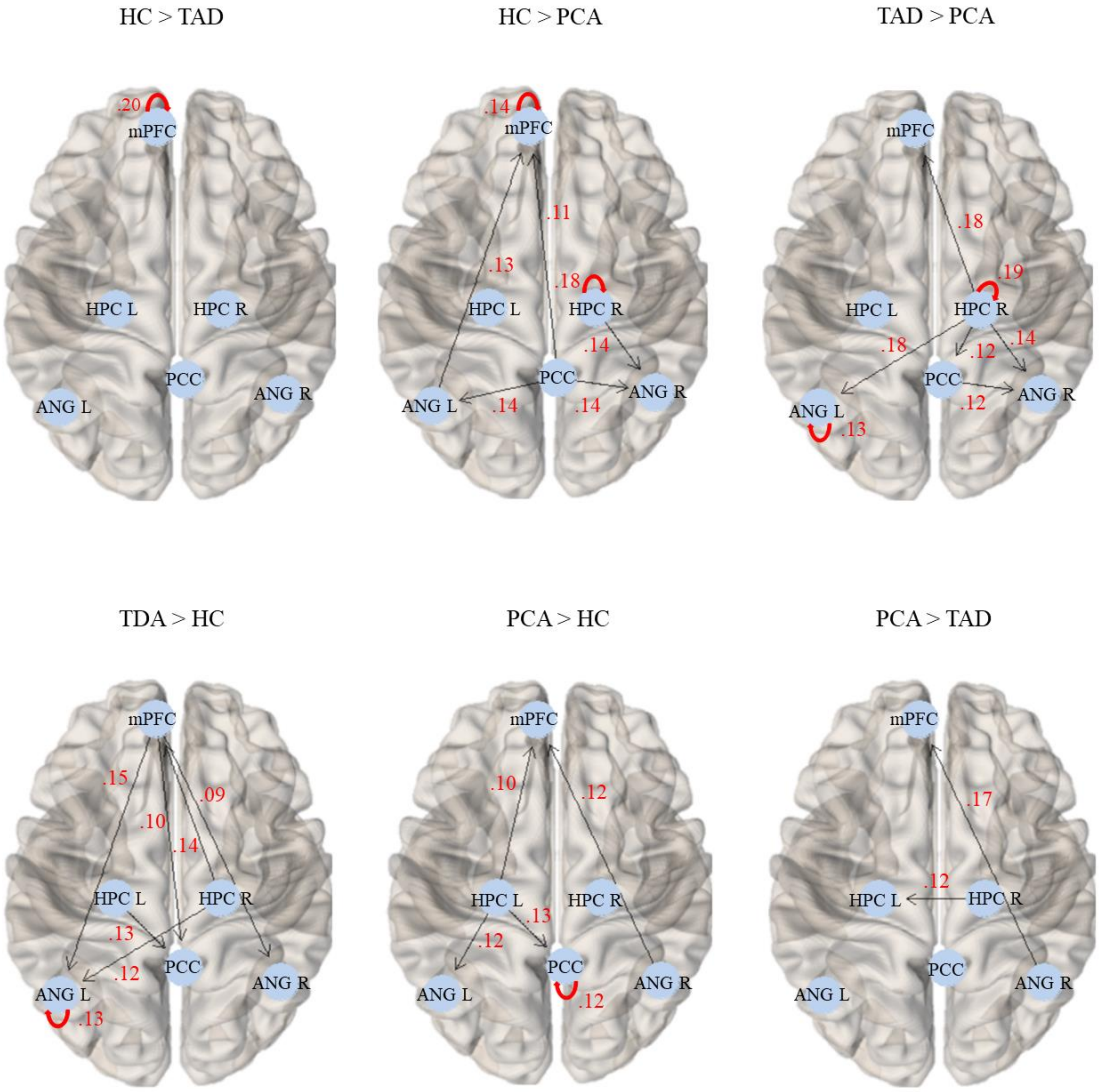

Figure 3. Group differences in DMN effective connectivity. Results were mapped on the brain using brainconn (https://github.com/sidchop/brainconn) implemented in R. Abbreviations: ANG, angular gyrus; HC, healthy controls; HPC, hippocampus; mPFC, medial prefrontal cortex; PCA, posterior cortical atrophy; PCC, posterior cingulate cortex, TAD, typical Alzheimer's disease.

Similarly, we identified higher input sensitivity of right middle frontal gyrus, higher connectivity from right middle frontal gyrus to other DMN regions (left middle frontal gyrus

and bilateral angular gyrus) and lower input sensitivity of right ANG in patients with typical AD compared to healthy controls in the ventral DMN (Figure S5).

PCA versus healthy controls

Similar to the patients with typical AD variant, patients with PCA exhibited lower mPFC self-connection (i.e., higher input sensitivity) compared to the healthy controls (Figure 3). The PCC-self connection was higher (i.e., lower input sensitivity) in the patients with PCA than the healthy controls. In addition, patients showed lower connectivity from PCC to other DMN regions (e.g., mPFC and bilateral ANG). Indeed, connections from PCC to bilateral ANG were excitatory in the healthy group, whereas they were missing or weakly inhibitory in the patients with PCA. Additionally, the patient group showed lower inhibitory connectivity from left HPC to mPFC, PCC and left ANG, lower right HPC self-connection, and higher inhibitory connectivity from right HPC to right ANG compared to the healthy controls.

Similarly, we identified higher input sensitivity of right middle frontal gyrus together with increased connectivity from right middle frontal gyrus to bilateral ANG and higher input sensitivity of right parahippocampal gyrus in patients with PCA compared to the healthy controls in the ventral DMN (Supplementary Fig. S5).

Typical AD versus PCA

Patients with typical AD had lower inhibitory right HPC connectivity to other DMN regions, and lower excitatory connectivity from right HPC to left HPC than the patients with PCA variant (Figure 3). Moreover, right HPC self-connection was higher in the typical AD group indicating lower sensitivity of the right HPC to input from other regions. Additionally, patients with typical AD exhibited lower left ANG self-connection, higher connectivity from PCC to right ANG (i.e., excitatory in the amnestic group) and lower connectivity from right ANG to mPFC (i.e., inhibitory in the amnestic group) compared the PCA group.

Similarly, we found that patients with typical AD exhibited lower input sensitivity of right parahippocampal gyrus and lower inhibitory connectivity from right parahippocampal gyrus to other DMN regions compared to the patients with PCA in the ventral DMN (Supplementary Fig. S5).

Brain-Behaviour Relationship

For the sake of simplicity, we report the brain-behaviour relationship only for the connections in which we found group differences. We found that both patient groups showed reduced mPFC self-inhibition (i.e., disinhibition) than the healthy controls. The mPFC self-connection was positively associated with cognitive scores in typical AD (β =0.22, *posterior probability* > 0.95). That is, mPFC disinhibition indicated lower cognitive performance in typical AD. No association was found for healthy participants and patients with PCA. Moreover, patients with typical AD exhibited increased connectivity from right HPC to right ANG (reduced inhibitory influence) compared to patients with PCA. The increased connectivity was associated with higher cognitive performance in typical AD patients (β =0.25, *posterior probability* > 0.95).

Additionally, we found that patients with PCA showed lower connectivity from PCC to mPFC and left ANG than the healthy controls. Lower connection strengths from PCC to mPFC (β =-0.22, *posterior probability* > 0.95) and left ANG (β =-0.15, *posterior probability* > 0.95) were associated with higher cognitive scores in patients with PCA.

Compared to patients with typical AD, patients with PCA had lower connectivity from right HPC to mPFC and left ANG. The lower connection strengths from right HPC to mPFC (β =-0.23, *posterior probability* > 0.95) and left ANG (β =-0.23, *posterior probability* > 0.95) were associated higher cognitive scores in patients with PCA, whereas no association was identified in the typical AD group.

These significant effects of cognitive scores on effective connectivity are important because they speak to the validity of the effective connectivity estimates; in the sense that the behavioural data were independent of the physiological data used to estimate connectivity.

Discussion

We here investigated effective connectivity within the DMN in two young-onset AD variants and healthy elderly to identify disease and variant-specific network alterations in the DMN. Our results indicated that both patient groups exhibited increased mPFC sensitivity to afferent inputs and a reduced inhibitory influence from left HPC to PCC, in comparison to healthy participants. Patients with typical AD uniquely showed excitatory connectivity from mPFC to posterior DMN nodes compared to healthy participants, whereas patients with PCA exhibited decreased connectivity from PCC to other DMN nodes and reduced inhibitory influence from left HPC to other DMN nodes. The connectivity of right hippocampus differentiated the patient groups.

Excitatory influences from prefrontal cortex to posterior DMN in typical AD variant

Reduced DMN functional connectivity is one of the most replicated findings in late-onset AD [10,48–54].In line with this, we hypothesized that the patients with typical AD would show decreased DMN connectivity compared to healthy participants. However, we did not identify decreased connectivity between DMN in patients with typical AD. On the contrary, we found that patients with typical AD had unique excitatory efferent connections from mPFC to posterior DMN nodes, which were missing in healthy controls and lower inhibitory influence from hippocampus to other DMN nodes. However, it is important to note that there is no one-to-one mapping between functional and effective connectivity. Indeed, they can be profound quantitative and qualitative differences between functional and effective connectivity [39]. This

follows from the fact that a change in one effective (directed) connection can change the correlations throughout the network—and therefore cause distributed changes in functional connectivity. Furthermore, functional connectivity cannot localise changes in self-connections (i.e., intrinsic connectivity) because the correlation of a region with itself is always one. We present the group mean functional connectivity in supplementary material (Supplementary Fig. S3) for comparison with the effective connectivity estimates in Figure 2.

Although most of the studies conducted in late-onset AD found reduced functional connectivity in patients compared to healthy elderly, the studies conducted with young-onset AD patients reported both decreased [16,18,55] and increased [16,19,56] resting-state functional connectivity in young-onset AD patients. In addition, increased functional connectivity in DMN can be component specific. Several studies identified increased DMN functional connectivity in anterior DMN in late-onset [11,57,58] and young-onset [19] AD. However, the definition of anterior DMN is not clear. Some studies defined anterior DMN by including only frontal areas [19,59], whereas others included some posterior areas in addition to frontal areas [11,60–62].

To exclude the possibility that our results were driven by the component choice, we repeated the same analysis using the ventral DMN. Importantly, both DMN components in the current study included frontal and parietal regions. However, the dorsal DMN contained the medial prefrontal region, whereas the ventral DMN contained lateral prefrontal regions. Independent from the component, we here identified increased input sensitivity of frontal regions and increased inter-regional effective connectivity from frontal regions to posterior nodes. Additionally, this pattern was not seen only in the typical AD variant but also in the PCA. Taken together, these results suggest that increased frontal cortex connectivity is related to disease pathology rather than the heterogeneity of DMN.

However, the meaning of increased connectivity is not clear. Some authors interpret the increased connectivity as an early compensatory mechanism in response to the loss of

functional capacity [58,63]. However, we here found that increased mPFC input sensitivity was associated with lower cognitive performance in typical AD patients, which does not support a compensatory mechanism. Moreover, damage to a neural system may also result in increased connectivity within and between network nodes [64]. This phenomenon has been documented in several neurodegenerative disorders including Parkinson's disease, multiple sclerosis, and mild cognitive impairment [63–66]. Although hyperconnectivity can be adaptive in the short-term, chronic hyperconnectivity may make the neural system vulnerable to secondary pathological processes [64].

Aβ-induced hyperexcitability can be a plausible explanation for the disinhibition findings in the current study. Aβ deposition is a well-documented neuropathological feature of AD. Animal studies showed that elevated Aß deposition induces neuronal hyperexcitability and triggers epileptiform activity in the hippocampal and cortical network in AD [67–69]. Another striking finding is the high prevalence rate of epileptic seizures in AD, especially young-onset AD [70–72]. Nonconvulsive seizures without clinical symptoms may be frequent in AD, especially those with younger age [73–75] and may be responsible for amnestic wandering and disorientation in patients with AD [71,74].

Importantly, brain regions showing Aß deposition are located within DMN [8,76]. Although Aß is widely used to explain neural hyperexcitability, the effect of Aß on functional connectivity is not clear [77]. Some studies showed that Aß leads to decreases in functional connectivity between network nodes [78–81], while others showed the other way around [82,83]. Tau protein might also play a role in the increased DMN connectivity in young-onset AD. A previous study showed a link between tau deposition and younger AD onset [84]. Moreover, increased anterior-posterior connectivity was found to be associated with increases in frontal tau deposition over time [85,86]. However, some other studies reported decreased connectivity related to tau deposition [77]. Unfortunately, we did not collect any neuropathological data to examine how protein deposition can be related to network alterations in young-onset AD.

Therefore, this explanation remains speculative. However, DCM can be a promising method to combine with neuropathological data, in future, to investigate whether enhanced excitatory or reduced inhibitory signalling is related to protein deposition in AD.

Patients with PCA exhibited both increased and decreased connectivity within DMN

Similar to the patients with typical AD, we hypothesized that the patients with PCA would exhibit reduced effective connectivity between DMN nodes compared to healthy participants. Our hypothesis was partially confirmed for the PCA variant. Healthy participants exhibited excitatory connections from PCC to mPFC and bilateral ANG indicating network integrity of DMN. However, patients with PCA either exhibited inhibitory influences from PCC to the other nodes or lack of outgoing efferent PCC connections. The PCC was also less sensitive to inputs of other DMN regions in patients with PCA than the healthy controls. These results were in line with our hypothesis claiming that patients with PCA would show more impairments in the connectivity of parietal regions. Several previous studies reported structural [6,87], functional [88] and connectomic [19,89] parietal cortex abnormalities in patients with PCA. Moreover, previous studies have also found decreased DMN functional connectivity in patients with PCA [20,87], which is compatible with our findings.

However, it is important to note that patients with PCA did not show only decreased effective connectivity. The effective connectivity from right ANG gyrus to mPFC was weakly excitatory in patients with PCA, whereas the same connection was inhibitory in healthy elderly and patients with typical AD. In addition, we identified a reduced inhibitory influence from left HPC to mPFC, left ANG and PCC than the healthy controls, which can be interpreted as a disinhibitory effect. This also shows that network alterations were not restricted to parietal regions in patients with PCA. Although medial temporal regions are relatively spared in PCA

[6], patients with PCA showed structural abnormalities in HPC compared to healthy elderly [5]. In addition to structural changes, a recent study using graph theory identified connectome abnormalities in the temporal cortex in patients with PCA [89]. Their findings showed that patients with PCA had lower local efficiency, lower nodal strength, lower clustering coefficient and higher path length in temporal regions than the healthy controls. Taken together, these results indicate that although the connectivity of parietal regions plays a more important role in PCA, the network alterations are not limited to parietal regions.

Right hippocampus connectivity differentiated young-onset AD variants

Patients with typical AD had reduced inhibitory connectivity from right hippocampus to other DMN regions compared to the patients with PCA. Additionally, the right HPC was less sensitive to inputs of other DMN regions and had a reduced excitatory outgoing connection to the left HPC in the typical AD variant. Our replication analysis also showed that similar results were found for the right parahippocampal gyrus in the ventral DMN. These results confirm that brain regions related to episodic memory functions are affected more in typical amnestic AD than PCA.

HPC is an important brain region for memory and learning and one of the earliest affected brain regions in AD [42]. Although both patient groups show grey matter abnormalities in the HPC, the differences are less in patients with PCA compared to patients with typical AD [5,90]. Therefore, group differences in hippocampal connectivity between the two young-onset AD variants can be expected. However, it is not clear why we found the group differences, specifically in the right hemisphere. A previous study reported higher total right hippocampus volume in patients with PCA than the patients with typical AD [88]. However, another study found left-sided group differences in hippocampus subfield volumes between the two AD variants [5]. In addition, to the best of our knowledge, there is no previous study comparing AD

variants in terms of hippocampus connectivity. The lack of previous empirical studies thus makes the interpretation of the results difficult.

Moreover, we found that alterations in right hippocampus effective connectivity were associated with higher cognitive performance in the two patient groups. Higher inhibitory influence from right HPC to mPFC and left ANG was associated with higher cognitive performance in patients with PCA, whereas the reduced inhibitory influence from right HPC to right ANG was associated with higher cognitive scores in patients with typical AD. These results indicate that right hippocampus connectivity can offer a compensatory mechanism to the young-onset AD variants in different directions.

Limitations

This study has several limitations that should be noted. First, our sample included only typical and PCA variants of AD. Investigating disease and variant-specific network alterations in other atypical AD variants such as logopenic progressive aphasia and behavioral AD could furnish new insights. Additionally, although comparable to the previous studies, our sample included fewer PCA cases (n=13), which can lead to reduced power in statistical analyses. Second, we did not measure Aβ or tau levels across the brain. We suggest that future studies should include neuropathological measurements to explain pathology behind the changes in the functional brain architectures. Third, the current study was cross-sectional. Longitudinal studies are needed to show how effective connectivity within and between networks change with disease progression.

Conclusion

We here investigated disease- and variant-specific alterations in the DMN connectivity in two common young-onset AD variants using spectral DCM. Our results indicated that the resting-

state DMN effective connectivity is a sensitive measure to detect disease- as well as variant-specific alterations in young-onset AD. However, since it was the first effective connectivity study in patients with young-onset AD variants, further research is needed to replicate these results.

Data availability

The data that support the findings of this study are available from the corresponding author, upon reasonable request.

Acknowledgements

The authors thank all study participants for their contribution in scientific advance.

Funding

The YOAD study was funded by Alzheimer's Research UK through a generous donation from Iceland Foods.

AR and KJF are affiliated with The Wellcome Centre for Human Neuroimaging, supported by core funding from Wellcome [203147/Z/16/Z]. AR is a CIFAR Azrieli Global Scholar in the Brain, Mind & Consciousness Program. JMS acknowledges the support of the National Institute for Health Research University College London Hospitals Biomedical Research Centre, Wolfson Foundation, Alzheimer's Research UK, Brain Research UK, Weston Brain Institute, Medical Research Council, British Heart Foundation, UK Dementia Research Institute and Alzheimer's Association. A.R. is funded by the Australian Research Council (Ref: DP200100757) and the Australian National Health and Medical Research Council (Investigator Grant 1194910). RWP acknowledges support from the National Institute for Health Research University College London Hospitals Biomedical Research Centre, the Alzheimer's Association. SC acknowledges the support of the Economic and Social Research Council and

National Institute for Health Research (ESRC/NIHR ES/L001810/1). K. Y. is an Etherington PCA Senior Research Fellow and is funded by the Alzheimer's Society, grant number 453 (AS-JF-18–003).

Competing interests

The authors declared no competing interests.

References

1. Mendez MF. Early-Onset Alzheimer Disease. *Neurol Clin*. Published online 2017. doi:10.1016/j.ncl.2017.01.005
2. Tellechea P, Pujol N, Esteve-Belloch P, et al. Early- and late-onset Alzheimer disease: Are they the same entity? *Neurologia*. 2018;33(4). doi:10.1016/j.nrl.2015.08.002
3. Graff-Radford J, Yong KXX, Apostolova LG, et al. New insights into atypical Alzheimer's disease in the era of biomarkers. *Lancet Neurol*. 2021;20(3). doi:10.1016/S1474-4422(20)30440-3
4. van der Flier WM, Pijnenburg YAL, Fox NC, Scheltens P. Early-onset versus late-onset Alzheimer's disease: The case of the missing APOE ε4 allele. *Lancet Neurol*. 2011;10(3). doi:10.1016/S1474-4422(10)70306-9
5. Parker TD, Slattery CF, Zhang J, et al. Cortical microstructure in young onset Alzheimer's disease using neurite orientation dispersion and density imaging. *Hum Brain Mapp*. 2018;39(7). doi:10.1002/hbm.24056
6. Warren JD, Fletcher PD, Golden HL. The paradox of syndromic diversity in Alzheimer disease. *Nat Rev Neurol*. 2012;8(8). doi:10.1038/nrneurol.2012.135
7. Bressler SL, Menon V. Large-scale brain networks in cognition: emerging methods and principles. *Trends Cogn Sci*. 2010;14(6). doi:10.1016/j.tics.2010.04.004

8. Buckner RL, Sepulcre J, Talukdar T, et al. Cortical hubs revealed by intrinsic functional connectivity: Mapping, assessment of stability, and relation to Alzheimer's disease. *J Neurosci*. 2009;29(6). doi:10.1523/JNEUROSCI.5062-08.2009

9. Buckner RL, Snyder AZ, Shannon BJ, et al. Molecular, structural, and functional characterization of Alzheimer's disease: Evidence for a relationship between default activity, amyloid, and memory. *J Neurosci*. 2005;25(34). doi:10.1523/JNEUROSCI.2177-05.2005

10. Greicius MD, Srivastava G, Reiss AL, Menon V. Default-mode network activity distinguishes Alzheimer's disease from healthy aging: Evidence from functional MRI. *Proc Natl Acad Sci U S A*. 2004;101(13). doi:10.1073/pnas.0308627101

11. Jones DT, MacHulda MM, Vemuri P, et al. Age-related changes in the default mode network are more advanced in Alzheimer disease. *Neurology*. 2011;77(16). doi:10.1212/WNL.0b013e318233b33d

12. Gili T, Cercignani M, Serra L, et al. Regional brain atrophy and functional disconnection across Alzheimer's disease evolution. *J Neurol Neurosurg Psychiatry*. 2011;82(1). doi:10.1136/jnnp.2009.199935

13. Celebi O, Uzdogan A, Oguz KK, et al. Default mode network connectivity is linked to cognitive functioning and CSF Aβ1-42 levels in Alzheimer's disease. *Arch Gerontol Geriatr*. 2016;62. doi:10.1016/j.archger.2015.09.010

14. Scherr M, Pasquini L, Benson G, et al. Decoupling of Local Metabolic Activity and Functional Connectivity Links to Amyloid in Alzheimer's Disease. *J Alzheimer's Dis*. 2018;64(2). doi:10.3233/JAD-180022

15. Huang J, Jung JY, Nam CS. Estimating effective connectivity in Alzheimer's disease progression: A dynamic causal modeling study. *Front Hum Neurosci*. 2022;16. doi:10.3389/fnhum.2022.1060936

16. Gour N, Felician O, Didic M, et al. Functional connectivity changes differ in early and

late-onset alzheimer's disease. *Hum Brain Mapp*. 2014;35(7). doi:10.1002/hbm.22379

17. Scherr M, Utz L, Tahmasian M, et al. Effective connectivity in the default mode network is distinctively disrupted in Alzheimer's disease—A simultaneous resting-state FDG-PET/fMRI study. *Hum Brain Mapp*. 2021;42(13). doi:10.1002/hbm.24517
18. Park KH, Noh Y, Choi EJ, Kim H, Chun S, Son YD. Functional connectivity of the hippocampus in early- and vs. late-onset alzheimer's disease. *J Clin Neurol*. 2017;13(4). doi:10.3988/jcn.2017.13.4.387
19. Lehmann M, Madison C, Ghosh PM, et al. Loss of functional connectivity is greater outside the default mode network in nonfamilial early-onset Alzheimer's disease variants. *Neurobiol Aging*. 2015;36(10). doi:10.1016/j.neurobiolaging.2015.06.029
20. Singh NA, Martin PR, Graff-Radford J, et al. Altered within- and between-network functional connectivity in atypical Alzheimer's disease. *Brain Commun*. 2023;5(4). doi:10.1093/braincomms/fcad184
21. McKhann GM, Knopman DS, Chertkow H, et al. The diagnosis of dementia due to Alzheimer's disease: Recommendations from the National Institute on Aging-Alzheimer's Association workgroups on diagnostic guidelines for Alzheimer's disease. *Alzheimer's Dement*. 2011;7(3). doi:10.1016/j.jalz.2011.03.005
22. Tang-Wai DF, Graff-Radford NR, Boeve BF, et al. Clinical, genetic, and neuropathologic characteristics of posterior cortical atrophy. *Neurology*. 2004;63(7). doi:10.1212/01.WNL.0000140289.18472.15
23. Power JD, Mitra A, Laumann TO, Snyder AZ, Schlaggar BL, Petersen SE. Methods to detect, characterize, and remove motion artifact in resting state fMRI. *Neuroimage*. Published online 2014. doi:10.1016/j.neuroimage.2013.08.048
24. Folstein MF, Folstein SE, McHugh PR. "Mini-mental state". A practical method for grading the cognitive state of patients for the clinician. *J Psychiatr Res*. Published online 1975. doi:10.1016/0022-3956(75)90026-6

25. Warrington EK. *Manual for the Recognition Memory Test for Words and Faces.* NFER- Nelson,; 1984.

26. Jackson M, Warrington EK. Arithmetic Skills in Patients with Unilateral Cerebral Lesions. *Cortex*. Published online 1986. doi:10.1016/S0010-9452(86)80020-X

27. Baxter DM, Warrington EK. Measuring dysgraphia: A graded-difficulty spelling test. *Behav Neurol*. 1994;7. doi:https://doi.org/10.3233/BEN-1994-73-401

28. Warrington EK, James M. *The Visual Object and Space Perception Battery*.; 1991. doi:10.1109/TVCG.2003.1196007

29. Delis DC, Kaplan E, Kramer JH. Delis-Kaplan executive function scale. . *San Antonio, TX Psychol Corp*. Published online 2001. doi:10.3109/02770903.2012.715704

30. Lin QH, Liu J, Zheng YR, Liang H, Calhoun VD. Semiblind spatial ICA of fMRI using spatial constraints. *Hum Brain Mapp*. 2010;31(7). doi:10.1002/hbm.20919

31. Goulden N, Khusnulina A, Davis NJ, et al. The salience network is responsible for switching between the default mode network and the central executive network: Replication from DCM. *Neuroimage*. 2014;99. doi:10.1016/j.neuroimage.2014.05.052

32. Chand GB, Wu J, Hajjar I, Qiu D. Interactions of insula subdivisions-based networks with default-mode and central-executive networks in mild cognitive impairment. *Front Aging Neurosci*. 2017;9(NOV). doi:10.3389/fnagi.2017.00367

33. Chand GB, Wu J, Hajjar I, Qiu D. Interactions of the Salience Network and Its Subsystems with the Default-Mode and the Central-Executive Networks in Normal Aging and Mild Cognitive Impairment. *Brain Connect*. 2017;7(7). doi:10.1089/brain.2017.0509

34. Stoliker D, Novelli L, Vollenweider FX, Egan GF, Preller KH, Razi A. Effective Connectivity of Functionally Anticorrelated Networks Under Lysergic Acid Diethylamide. *Biol Psychiatry*. 2023;93(3). doi:10.1016/j.biopsych.2022.07.013

35. Shirer WR, Ryali S, Rykhlevskaia E, Menon V, Greicius MD. Decoding subject-driven

cognitive states with whole-brain connectivity patterns. *Cereb Cortex*. Published online 2012. doi:10.1093/cercor/bhr099

36. Pievani M, Pini L, Ferrari C, et al. Coordinate-Based Meta-Analysis of the Default Mode and Salience Network for Target Identification in Non-Invasive Brain Stimulation of Alzheimer's Disease and Behavioral Variant Frontotemporal Dementia Networks. *J Alzheimer's Dis*. 2017;57(3). doi:10.3233/JAD-161105
37. Razi A, Kahan J, Rees G, Friston KJ. Construct validation of a DCM for resting state fMRI. *Neuroimage*. 2015;106. doi:10.1016/j.neuroimage.2014.11.027
38. Friston KJ, Kahan J, Biswal B, Razi A. A DCM for resting state fMRI. *Neuroimage*. Published online 2014. doi:10.1016/j.neuroimage.2013.12.009
39. Novelli L, Friston KJ, Razi A. Spectral Dynamic Causal Modelling: A Didactic Introduction and its Relationship with Functional Connectivity. *Netw Neurosci*. Published online 2023. doi:https://doi.org/10.1162/netn_a_00348
40. Friston KJ, Litvak V, Oswal A, et al. Bayesian model reduction and empirical Bayes for group (DCM) studies. *Neuroimage*. Published online 2016. doi:10.1016/j.neuroimage.2015.11.015
41. Zeidman P, Jafarian A, Seghier ML, et al. A tutorial on group effective connectivity analysis, part 2 : second level analysis with PEB 1 Introduction. *Arxiv*. Published online 2019.
42. Mu Y, Gage FH. Adult hippocampal neurogenesis and its role in Alzheimer's disease. *Mol Neurodegener*. 2011;6(1). doi:10.1186/1750-1326-6-85
43. Damoiseaux JS, Beckmann CF, Arigita EJS, et al. Reduced resting-state brain activity in the "default network" in normal aging. *Cereb Cortex*. 2008;18(8). doi:10.1093/cercor/bhm207
44. Andrews-Hanna JR, Reidler JS, Sepulcre J, Poulin R, Buckner RL. Functional-Anatomic Fractionation of the Brain's Default Network. *Neuron*. 2010;65(4).

doi:10.1016/j.neuron.2010.02.005

45. Guan Z, Zhang M, Zhang Y, Li B, Li Y. Distinct Functional and Metabolic Alterations of DMN Subsystems in Alzheimer's Disease: A Simultaneous FDG-PET/fMRI Study. In: *Proceedings of the Annual International Conference of the IEEE Engineering in Medicine and Biology Society, EMBS*. ; 2021. doi:10.1109/EMBC46164.2021.9629472

46. Friston KJ, Harrison L, Penny W. Dynamic causal modelling. *Neuroimage*. Published online 2003. doi:10.1016/S1053-8119(03)00202-7

47. Zeidman P, Jafarian A, Corbin N, et al. A guide to group effective connectivity analysis, part 1: First level analysis with DCM for fMRI. *Neuroimage*. 2019;200(March):174-190. doi:10.1016/j.neuroimage.2019.06.031

48. Balachandar R, John JP, Saini J, et al. A study of structural and functional connectivity in early Alzheimer's disease using rest fMRI and diffusion tensor imaging. *Int J Geriatr Psychiatry*. 2015;30(5). doi:10.1002/gps.4168

49. Brier MR, Thomas JB, Snyder AZ, et al. Loss of intranetwork and internetwork resting state functional connections with Alzheimer's disease progression. *J Neurosci*. 2012;32(26). doi:10.1523/JNEUROSCI.5698-11.2012

50. Dai Z, Yan C, Li K, et al. Identifying and mapping connectivity patterns of brain network hubs in Alzheimer's disease. *Cereb Cortex*. 2015;25(10). doi:10.1093/cercor/bhu246

51. Liu Z, Zhang Y, Bai L, et al. Investigation of the effective connectivity of resting state networks in Alzheimer's disease: A functional MRI study combining independent components analysis and multivariate Granger causality analysis. *NMR Biomed*. 2012;25(12). doi:10.1002/nbm.2803

52. Teipel SJ, Metzger CD, Brosseron F, et al. Multicenter resting state functional connectivity in prodromal and dementia stages of Alzheimer's disease. *J Alzheimer's Dis*. 2018;64(3). doi:10.3233/JAD-180106

53. Zhou J, Greicius MD, Gennatas ED, et al. Divergent network connectivity changes in behavioural variant frontotemporal dementia and Alzheimer's disease. *Brain*. 2010;133(5). doi:10.1093/brain/awq075

54. Zhu H, Zhou P, Alcauter S, et al. Changes of intranetwork and internetwork functional connectivity in Alzheimer's disease and mild cognitive impairment. *J Neural Eng*. 2016;13(4). doi:10.1088/1741-2560/13/4/046008

55. Adriaanse SM, Binnewijzend MAA, Ossenkoppele R, et al. Widespread disruption of functional brain organization in early-onset Alzheimer's disease. *PLoS One*. 2014;9(7). doi:10.1371/journal.pone.0102995

56. Fide E, Hünerli-Gündüz D, Öztura İ, Yener GG. Hyperconnectivity matters in early-onset Alzheimer's disease: a resting-state EEG connectivity study. *Neurophysiol Clin*. 2022;52(6). doi:10.1016/j.neucli.2022.10.003

57. Sanz-Arigita EJ, Schoonheim MM, Damoiseaux JS, et al. Loss of "Small-World" Networks in Alzheimer's Disease: Graph Analysis of fMRI Resting-State Functional Connectivity. *PLoS One*. 2010;5(11). doi:10.1371/journal.pone.0013788

58. Cha J, Jo HJ, Kim HJ, et al. Functional alteration patterns of default mode networks: Comparisons of normal aging, amnestic mild cognitive impairment and Alzheimer's disease. *Eur J Neurosci*. 2013;37(12). doi:10.1111/ejn.12177

59. Dipasquale O, Griffanti L, Clerici M, Nemni R, Baselli G, Baglio F. High-dimensional ica analysis detects within-network functional connectivity damage of default-mode and sensory-motor networks in alzheimer's disease. *Front Hum Neurosci*. 2015;9(FEB). doi:10.3389/fnhum.2015.00043

60. Damoiseaux JS, Prater KE, Miller BL, Greicius MD. Functional connectivity tracks clinical deterioration in Alzheimer's disease. *Neurobiol Aging*. 2012;33(4). doi:10.1016/j.neurobiolaging.2011.06.024

61. Li B, Liu L, Friston KJ, et al. A treatment-resistant default mode subnetwork in major

depression. *Biol Psychiatry*. 2013;74(1). doi:10.1016/j.biopsych.2012.11.007

62. Sambataro F, Wolf ND, Pennuto M, Vasic N, Wolf RC. Revisiting default mode network function in major depression: Evidence for disrupted subsystem connectivity. *Psychol Med*. 2014;44(10). doi:10.1017/S0033291713002596

63. Qi Z, Wu X, Wang Z, et al. Impairment and compensation coexist in amnestic MCI default mode network. *Neuroimage*. 2010;50(1). doi:10.1016/j.neuroimage.2009.12.025

64. Hillary FG, Grafman JH. Injured Brains and Adaptive Networks: The Benefits and Costs of Hyperconnectivity. *Trends Cogn Sci*. 2017;21(5). doi:10.1016/j.tics.2017.03.003

65. Gardini S, Venneri A, Sambataro F, et al. Increased Functional Connectivity in the Default Mode Network in Mild Cognitive Impairment: A Maladaptive Compensatory Mechanism Associated with Poor Semantic Memory Performance. *J Alzheimer's Dis*. 2015;45(2). doi:10.3233/JAD-142547

66. Jacobs HIL, Van Boxtel MPJ, Heinecke A, et al. Functional integration of parietal lobe activity in early Alzheimer disease. *Neurology*. 2012;78(5). doi:10.1212/WNL.0b013e318245287d

67. Hazra A, Gu F, Aulakh A, Berridge C, Eriksen JL, Žiburkus J. Inhibitory Neuron and Hippocampal Circuit Dysfunction in an Aged Mouse Model of Alzheimer's Disease. *PLoS One*. 2013;8(5). doi:10.1371/journal.pone.0064318

68. Minkeviciene R, Rheims S, Dobszay MB, et al. Amyloid β-induced neuronal hyperexcitability triggers progressive epilepsy. *J Neurosci*. 2009;29(11). doi:10.1523/JNEUROSCI.5215-08.2009

69. Palop JJ, Chin J, Roberson ED, et al. Aberrant Excitatory Neuronal Activity and Compensatory Remodeling of Inhibitory Hippocampal Circuits in Mouse Models of Alzheimer's Disease. *Neuron*. 2007;55(5). doi:10.1016/j.neuron.2007.07.025

70. Irizarry MC, Jin S, He F, et al. Incidence of new-onset seizures in mild to moderate Alzheimer disease. *Arch Neurol*. 2012;69(3). doi:10.1001/archneurol.2011.830

71. Palop JJ, Mucke L. Epilepsy and cognitive impairments in alzheimer disease. *Arch Neurol*. 2009;66(4). doi:10.1001/archneurol.2009.15

72. Scarmeas N, Honig LS, Choi H, et al. Seizures in Alzheimer disease: Who, when, and how common? *Arch Neurol*. 2009;66(8). doi:10.1001/archneurol.2009.130

73. Horváth A, Szcs A, Barcs G, Noebels JL, Kamondi A. Epileptic Seizures in Alzheimer Disease. *Alzheimer Dis Assoc Disord*. 2016;30(2). doi:10.1097/WAD.0000000000000134

74. Vossel KA, Tartaglia MC, Nygaard HB, Zeman AZ, Miller BL. Epileptic activity in Alzheimer's disease: causes and clinical relevance. *Lancet Neurol*. 2017;16(4). doi:10.1016/S1474-4422(17)30044-3

75. Vossel KA, Beagle AJ, Rabinovici GD, et al. Seizures and epileptiform activity in the early stages of Alzheimer disease. *JAMA Neurol*. 2013;70(9). doi:10.1001/jamaneurol.2013.136

76. Sperling RA, LaViolette PS, O'Keefe K, et al. Amyloid Deposition Is Associated with Impaired Default Network Function in Older Persons without Dementia. *Neuron*. 2009;63(2). doi:10.1016/j.neuron.2009.07.003

77. Hasani SA, Mayeli M, Salehi MA, Barzegar Parizi R. A systematic review of the association between amyloid-β and τ pathology with functional connectivity alterations in the alzheimer dementia spectrum utilizing PET Scan and rsfMRI. *Dement Geriatr Cogn Dis Extra*. 2021;11(2). doi:10.1159/000516164

78. Hedden T, Van Dijk KRA, Becker JA, et al. Disruption of functional connectivity in clinically normal older adults harboring amyloid burden. *J Neurosci*. 2009;29(40). doi:10.1523/JNEUROSCI.3189-09.2009

79. Kang DW, Choi WH, Jung WS, Um YH, Lee CU, Lim HK. Impact of Amyloid

Burden on Regional Functional Synchronization in the Cognitively Normal Older Adults. *Sci Rep*. 2017;7(1). doi:10.1038/s41598-017-15001-8

80. Song Z, Insel PS, Buckley S, et al. Brain amyloid-β burden is associated with disruption of intrinsic functional connectivity within the medial temporal lobe in cognitively normal elderly. *J Neurosci*. 2015;35(7). doi:10.1523/JNEUROSCI.2092-14.2015

81. Giorgio J, Adams JN, Maass A, Jagust WJ, Breakspear M. Amyloid induced hyperexcitability in default mode network drives medial temporal hyperactivity and early tau accumulation. *Neuron*. 2023;112. doi:DOI:https://doi.org/10.1016/j.neuron.2023.11.014

82. Schultz AP, Chhatwal JP, Hedden T, et al. Phases of hyperconnectivity and hypoconnectivity in the default mode and salience networks track with amyloid and tau in clinically normal individuals. *J Neurosci*. 2017;37(16). doi:10.1523/JNEUROSCI.3263-16.2017

83. Sepulcre J, Grothe MJ, Sabuncu M, et al. Hierarchical organization of tau and Amyloid deposits in the cerebral cortex. *JAMA Neurol*. 2017;74(7). doi:10.1001/jamaneurol.2017.0263

84. Frontzkowski L, Ewers M, Brendel M, et al. Earlier Alzheimer's disease onset is associated with tau pathology in brain hub regions and facilitated tau spreading. *Nat Commun*. 2022;13(1). doi:10.1038/s41467-022-32592-7

85. Katsumi Y, Putcha D, Eckbo R, et al. Anterior dorsal attention network tau drives visual attention deficits in posterior cortical atrophy. *Brain*. 2023;146(1). doi:10.1093/brain/awac245

86. Sintini I, Graff-Radford J, Jones DT, et al. Tau and Amyloid Relationships with Resting-state Functional Connectivity in Atypical Alzheimer's Disease. *Cereb Cortex*. 2021;31(3). doi:10.1093/cercor/bhaa319

87. Agosta F, Mandic-Stojmenovic G, Canu E, et al. Functional and structural brain networks in posterior cortical atrophy: A two-centre multiparametric MRI study. *NeuroImage Clin*. Published online 2018. doi:10.1016/j.nicl.2018.06.013

88. Peng G, Wang J, Feng Z, et al. Clinical and neuroimaging differences between posterior cortical atrophy and typical amnestic Alzheimer's disease patients at an early disease stage. *Sci Rep*. 2016;6. doi:10.1038/srep29372

89. Migliaccio R, Agosta F, Basaia S, et al. Functional brain connectome in posterior cortical atrophy. *NeuroImage Clin*. 2020;25. doi:10.1016/j.nicl.2019.102100

90. Manning EN, Macdonald KE, Leung KK, et al. Differential hippocampal shapes in posterior cortical atrophy patients: A comparison with control and typical AD subjects. *Hum Brain Mapp*. 2015;36(12):5123-5136. doi:10.1002/hbm.22999